

## Evaluation of Deflection-based Predictors for Estimating Thoracic Injury Risk

D. Bose<sup>1</sup>, J. R. Crandall<sup>1</sup>, B. Pipkorn<sup>2</sup>, E. Song<sup>3</sup>, Z. Li<sup>1</sup>, D. J. Lessley<sup>1</sup> and R. W. Kent<sup>1</sup>

<sup>1</sup> University of Virginia Center for Applied Biomechanics, Charlottesville, USA

<sup>2</sup> Autoliv Research, Vårgårda, Sweden

<sup>3</sup> LAB PSA Peugeot Citroën Renault, France

*This paper has not been screened for accuracy nor refereed by any body of scientific peers and should not be referenced in the open literature.*

### ABSTRACT

*Towards the development of a dummy-based thoracic injury risk function, previous studies have emphasized the need to determine an injury predictor variable derived from dummy deflection measurements such that the injury prediction is independent of the type of restraint loading. The goal of this study was to evaluate the significance of multi-point deflections measured on the anterior and lateral rib cage in predicting the risk of rib injury in different frontal crash loading scenarios. The methodology of the study included statistical analyses using regression techniques to correlate the risk of severe rib injury and maximum strain in the ribcage with linear combinations of multi-point deflections as explanatory predictors. Thoracic multi-point deflection data used for regression analyses included data from 20 sled tests involving belt restrained Post Mortem Test Subjects (PMHS) and simulation based thoracic deformation data involving two finite element human models oriented in 18 different loading conditions. The loading conditions for the simulation database included table top loading with 3 point belt, 4 point belt, airbag and hub restraints; static airbag and pendulum loading for seated occupant; and dynamic sled tests with belt only, airbag only and combined belt and airbag restraints. In addition to the evaluation of the deflection predictors, qualitative predictors, describing the loading environment, were evaluated including the presence of belt and airbag restraint, hub impact, and load-limiting restraining force. The results demonstrated that for frontal loading of the thorax by the 3 point belt system, the mid-sternum deflection and existing  $C_{max}$  measure performed better compared to the composite multi-point deflections in predicting the risk of severe rib injury in PMHS. The simulation results which characterized the thoracic deformation in different restraint loading conditions, loading rates and two different human models, suggested that lateral deflections in addition to the standard four point anterior deflections were significant to the prediction of the maximum strain in the rib cage. The linear combination of multi-point deflection predictors as derived in this study may be further modified to provide the framework for dummy-based injury risk function applicable to a range of standard restraint conditions in frontal crashes.*

## INTRODUCTION

Thoracic deflections measured by the Anthropometric Test Devices (ATD) have been traditionally used as predictors of chest injury risk in real world frontal motor vehicle collisions (Eppinger et al., 1999).

For instance, the posterior deflection of the mid-sternum relative to the spine measured by the Hybrid-III ATD, commonly referred to as chest deflection, has been shown to be a predictor for chest injury risk based on results from matched-pair comparisons involving ATD and PMHS tests (Kent et al., 2001). Chest deflection, however, characterizes the thoracic deformation at the mid-sternum location which, depending on the restraint type, may not correspond to the location of the maximum thoracic deflection (Kuppa & Eppinger 1998). Consequently, injury metrics like chest deflection which rely on deflection measured at a fixed location may have limited ability to discriminate injury from non-injury when different restraint loading types are considered and the injury prediction is further dependent on subject parameters including age, gender and anthropometry (cf. Kent & Patrie, 2005). With advances in ATD sensor technology (e.g., four point multi-axis thoracic deflection measured on the THOR ATD), thoracic deformation can be evaluated at multiple locations which should considerably improve the ability to distinguish injury under different loading conditions. To compare the sensitivity in injury prediction between multi-point thoracic deflection and fixed-location chest deflection to different restraint conditions, a matched-pair test analysis involving multi-point deflection measured on the THOR ATD and the PMHS injury outcome was previously performed by the authors (Figure 1). The correlation between the magnitude of maximum thoracic deflection measured at any of the four locations on the THOR,  $C_{max}$ , and the risk of severe thoracic injury, was evaluated to be dependent on the restraint type. It should be noted that a relatively smaller sample size ( $n=29$ ) was available to develop the injury risk function for the THOR ATD with restraint type broadly classified between belt only and belt and airbag combined loading. Further investigation into the association between the components of multipoint deflections and the risk of injury is necessary to develop an injury risk function independent of the restraint type.

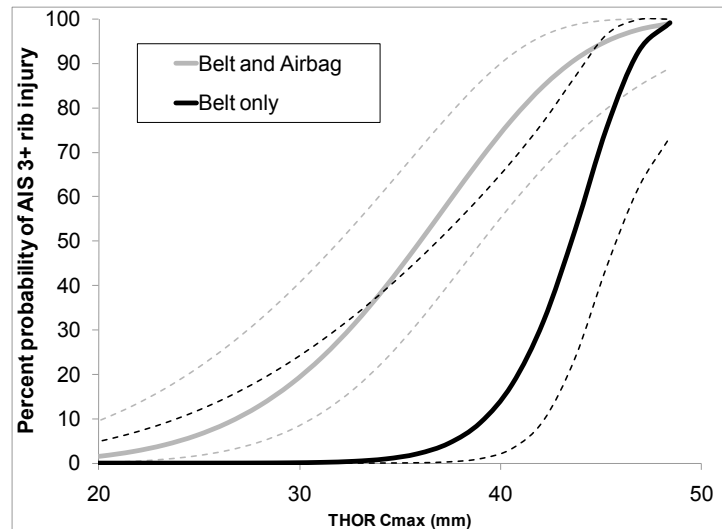


Figure 1: Sensitivity of the thoracic injury risk curve (for AIS 3+ rib injury) to restraint conditions based on matched-pair PMHS THOR sled test data. The injury risk curve is based on right-censored parametric (Weibull distribution) survival analysis (Maximum likelihood estimates) with superimposed 95% confidence interval (dashed lines) for each of the restraint types. *Figure adapted from Bose et al., 2009.*

While further improvements and validation of the dummy-based injury risk function is contingent upon additional matched-pair sled test data, a necessary prerequisite for the same goal is to establish a functional form of the multi-point deflection which can be used as an injury predictor in the risk function. Towards that goal, the objective of the current study was to analyze the correlation between multi-point deflections measured on the thoracic rib cage and the risk of rib injury measured during the deformation of the human thorax under a range of standard loading conditions using experimental and computationally simulated test results. Further, it has been assumed in the analysis that the risk of rib fracture injury at any instant of time during the thoracic deformation is independent of the spatial and temporal history of the

deformation state. This assumption neglects the effects of viscoelastic material properties of the rib cage and is in agreement with previously reported computational strategies used for modeling thoracic ribs (Li et al., 2009). Our research group at the University of Virginia (UVA) had previously conducted an extensive test matrix of PMHS sled tests with appropriate chest deflection instrumentation, the results of which provide multi-point chest deflections and corresponding post-test rib injury outcome. In the current study, the results from UVA database of PMHS sled tests have been used to correlate peak values of composite multi-point deflections with the incidence of severe rib injury as observed for each individual subject. The PMHS database while providing biofidelic data points for thoracic deflection and rib injury represents a limited number of restraint types and loading conditions. Additionally, it must be noted that in a PMHS test the timing (and the corresponding deflections) of the rib injury is censored or unknown during the thoracic deformation. To account for these shortcomings in the PMHS database, the current study also investigated thoracic deflection and risk of rib injury obtained from computational simulation of multiple human models. The simulations are representative of a wide range of previously performed experimental tests which include a matrix of different restraint types and loading rates. Finally, a variable reduction strategy for the predictor deflections was investigated in this study to identify principal components (Eigen vectors) and common factors among the nine multi-point deflections measured on the anterior and lateral thoracic rib cage. In summary, the task-based objectives towards the overall goal of the study are described as follows:

1. To evaluate and compare the peak values of composite multi-point deflections as predictors of severe rib injury risk using results from PMHS sled tests.
2. To develop a linear regression model to evaluate different linear combinations of multi-point deflection as predictors of overall maximum strain in the rib cage using simulation results of thoracic deformation involving a variety of restraint types—3 point belt, 4 point belt, airbag, 3 point belt and airbag, hub impactor—and different loading conditions—table top with supine subject, stationary seated subject, and dynamic sled test—performed at different severities of injury risk.
3. To analyze the principal components and common factors among the nine multi-point deflections measured on the anterior and lateral thoracic rib cage to be potentially used for defining the predictor function associated with the risk of rib injury

## METHODS

Multivariate regression analyses performed on thoracic deformation data, obtained from experimental PMHS sled tests and computational simulation of human thorax models, were used to estimate the effect of multi-point deflection data on the risk of rib injury. The thoracic deformation data in the experimental sled tests were evaluated using the chest-band instrumentation mounted at two different levels on the PMHS subjects. The binary injury outcome for these tests was quantified by the incidence of rib injury with Abbreviated Injury Score (AIS, for details refer to AAAM, 2005) of three or more (AIS 3+). Additionally, two previously validated Finite Element (FE) models of the human torso were used to simulate thoracic deformation in response to static and dynamic loading conditions. Static loading conditions, with the human torso held stationary before impact, were representative of four different vehicle restraint types: diagonal shoulder belt, frontal airbag represented as distributed load, steering wheel hub impactor at mid-sternum level and cross-over dual belt. The dynamic loading conditions involved simulating a human occupant restrained under different conditions (belt only, airbag only and combination of belt and airbag) in a sled at different impact speeds (40km/h to 60km/h). The outcome variable in the modeling results was the first peak principal strain measured in the overall rib cage.

For the injury-deflection data measured in the experimental sled tests, logistic regression analyses were performed to correlate scalar combinations of multi-point deflections, as injury predictors, with the outcome expressed as the incidence of AIS 3+ rib injury. Statistical measures were used to rank the predictors in terms of goodness of model fit, predictability, and statistical significance of model parameters. The strain-deflection data obtained from the simulations (18 different loading conditions involving two different human models) sampled at 1 kHz were considered as independent data points ignoring the temporal effects of the thoracic deformation as discussed previously. Linear regression models were used to evaluate the multi-point deflections as predictors of peak strain in the rib cage. Additionally, the correlations and common variance between the multi-point predictors was analyzed using Principal Component Analysis (PCA) and Common Factor Analysis (CFA).

The biomechanical dataset obtained from the experimental sled tests, computational modeling and the statistical analyses are described in the following subsections (Figure 2).

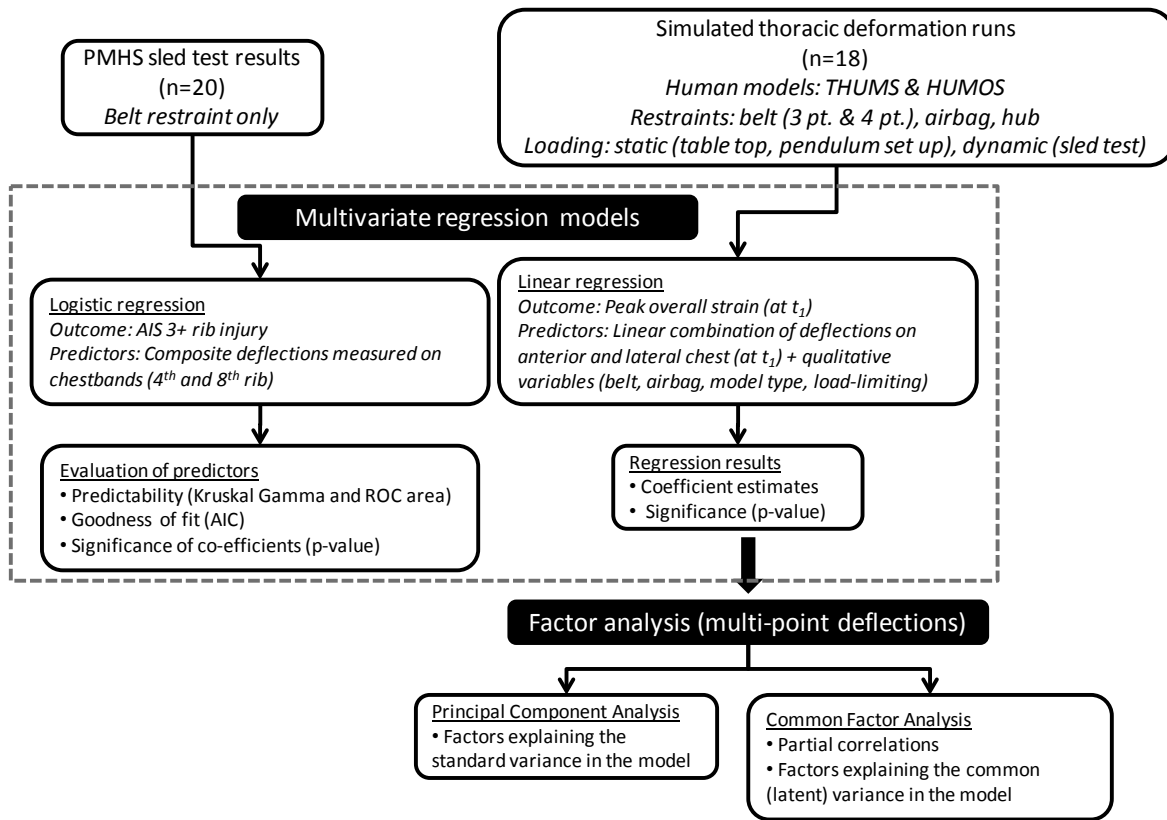


Figure 2: Summary of the study methodology.

## PMHS injury-deflection database

Thoracic multi-point deflection data from twenty sled tests involving PMHS subjects were analyzed in this study. The average±standard deviation age, stature, mass, and chest depth of the selected subjects (16 males, 4 females) were 55±10 years, 1.73±0.13 m, 80±37 kg, and 244±43mm respectively. The sled impact speeds were at 30km/h and 50km/h and the occupant restraints included a 3-point seat belt system (12 cases with buckle pretensioners and force-limiting retractors). The average number of rib fractures observed was 5.6 fractures per subject with 8 subjects sustaining AIS 3+ rib injury. Details about the PMHS subjects and the sled test conditions are available in Table A.1. The subjects were used in accordance with ethical guidelines and research protocol approved by the University of Virginia Institutional Review Board.

Multi-point thoracic deflection was measured for each of the PMHS subjects using chest-band instrumentation (Denton, USA) at the upper (4th rib) and lower (8th rib) chest levels. The chest-band is a curvature measurement device consisting of a flexible band of variable length with 52 active strain gauge bridges attached at fixed locations along the length of the band. Each strain gauge bridge continuously measures the strain at the location of the bridge, and thus local curvature information can be used to generate the actual physical shape of the chest band loop at that particular point in time. Curvature data from the two chest-bands were collected at 10,000 samples/sec using TRAQ-P, a DSP Technology Transient Acquisition and Processing System, and IMPAX, a DSP Technology PC-based data acquisition program. These collected curvature data were post-processed using Conrad Technologies, Inc. software (RBANDPC and DEFLECT v.3.0 (2001)) to produce chest band contours at selected time intervals throughout the impact event.

A deformation analysis was performed on the post-processed chest-band results to quantify thoracic deformation at three anterior locations on each of the chest-bands. The analysis was performed by establishing three separate line segments or chords (Left, Right, and Central illustrated in Figure 3). Each of the three chords (left, central, and right) was established as a pair of points (one anterior and one posterior). The left and right chords were positioned at a specified distance of 38 mm from the center-line of the contour. This selected lateral distance of 38 mm is commonly used in the analysis of PMHS chest-band data

and matches the anterior CRUX measurement locations in the THOR frontal Anthropometric Test Device (ATD) while the central (mid sternum) location matches the internal measurement location in the Hybrid III ATD. The peak values of deflection time histories at these six points on the anterior thorax were used as injury predictors in the study. The injury outcome was derived based on the rib fractures as observed during the post-test necropsy performed by an orthopedic surgeon. The number of rib fractures and their location was used to determine the incidence of AIS 3+ injury based on the guidelines provided in AIS injury coding manual (AAAM, 2005).

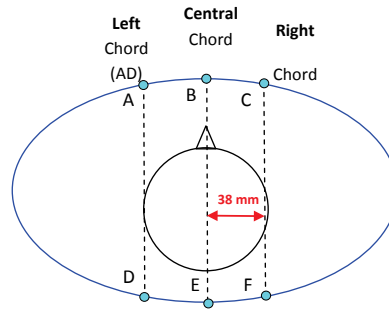


Figure 3: Chord measurement locations on the chest-band contour. The chord deformation (change in length) was measured at three anterior locations (center and 38mm laterally) for each of the chest-bands.

## Computational modeling

*Description of the torso FE models.* Two computational models of the human torso used in this study were obtained from the THUMS (Total Human Model for Safety) and the HUMOS (Human Model for Safety) whole body FE models. The THUMS model was developed and validated by the research team at Toyota Central R&D Labs, Inc., to simulate the human response to impact loads (Oshita et al., 2002). The anthropometry measures of the THUMS model are representative of the 50<sup>th</sup> percentile American adult male. The model includes detailed anatomical features including skeletal structures, soft tissue organs, muscle groups and skin structure modeled using a total of over sixty thousand nodes and eighty thousand elements. The thorax region of the THUMS model consists of the sternum, ribs, clavicles, and the scapula modeled using deformable elements while vertebrae are modeled as rigid-bodies. The cortical and trabecular bones are distinguished in terms of material property and modeled with shell and solid elements, respectively. The internal soft tissue organs were modeled as deformable solid elements with simplified geometrical properties. The computational time step for the thorax model is of the order of 1.0e-8 seconds. Further details about the THUMS thorax model are available in Murakami et al. (2004).

The HUMOS model is a full human body FE model developed by a consortium of universities, research groups and automotive industries (Vezin et al., 2005). The anthropometry of the model is representative of the 50<sup>th</sup> percentile adult European male. In the thorax region of the HUMOS model, the cortical bone of the ribs and the sternum was represented by shell elements, and the trabecular bone by solid elements. The cartilage between the sternum and the ribs was also represented by solid elements. The muscles and internal organs, such as the heart, lungs, stomach and liver were represented by solid elements. An elasto-plastic material law was used to model the cortical bone, an elastic material law for the trabecular bone and cartilage, and a Boltzman material law for the organs and muscles. The vertebrae were considered as rigid bodies, the connections between them were modeled with general springs. The same was done for the connections between the ribs and the vertebrae. Further details about the HUMOS model are available in Song et al., (2009).

*Loading conditions for thoracic deformation.* A range of restraint loading conditions were used to simulate thoracic deformation in the two human models. The supine THUMS torso model was oriented in the table-top orientation (for further details refer to Kent et al., 2004), with fixed displacement boundary conditions to the spine and the pelvic structure (Figure 4). The torso-back and the head were positioned against two planar structures at different levels to ensure stability with no anterior-posterior movement of the spinal structure due to the inertial forces of the head/neck complex and the pelvis structure. Simplified finite

element models of the four restraint types-driver side diagonal shoulder belt, deformable planar structure for distributed loading, rigid hub and cross-over dual belt-represented using deformable shell elements were used in the restraint loading simulation of the thorax (Figure 4). The kinematic boundary condition for the restraints to simulate a dynamic deformation of the thorax includes a constant velocity (1 m/s) displacement pulse with peak stroke of 46 mm corresponding to chest compression of 23% of its initial depth under diagonal belt loading. The choice of restraint kinematics relates to a nominal risk of sustaining rib fracture injuries from a belt restraint loading in a 48 km/hr frontal collision (Kent et al., 2004). The kinematic boundary conditions were applied to the restraint attachment points in the anterior-to-posterior direction of the torso model.

The HUMOS human model was oriented in three different loading conditions (Figure 5). The first condition replicated a pendulum impact test while the subject was in the seated posture (Kroell et al., 1971, Kroell et al., 1974). The second test configuration was representative of an out-of-position airbag deployment (driver-side module) while the subject was positioned as seated on a static test bench (refer to Lebarbé et al., 2005 for further details on the test set-up). The simulation matrix in this configuration included variation in the pre-impact distance between the airbag and the thorax. The third configuration was a dynamic sled test with the subject in a driver seat orientation restrained by different combinations of 3-point belt and airbag systems with varying values for impact speed, load limiting force and airbag mass flow rate (Petitjean et al., 2002). The set-up of the HUMOS model in the three test configurations is shown in Figure 5. A complete list of simulation test matrix involving both human models is presented in Table 1.

Table 1: Test matrix for simulating thoracic deformation using multiple human models

Simulation number	Human model	Test condition	Restraint type	Loading condition
1	THUMS	Table top	3 point belt	Peak loading velocity=1m/s
2	THUMS	Table top	Airbag	Peak loading velocity=1m/s
3	THUMS	Table top	4 point belt	Peak loading velocity=1m/s
4	THUMS	Table top	Hub impactor	Peak loading velocity=1m/s
5	HUMOS	Sled	3 point belt	Impact speed=40km/h, belt load limit=6kN
6	HUMOS	Sled	3 point belt	Impact speed=45km/h, belt load limit=6kN
7	HUMOS	Sled	3 point belt	Impact speed=50km/h, belt load limit=6kN
8	HUMOS	Sled	3 point belt and airbag	Impact speed=40km/h, belt load limit=4kN
9	HUMOS	Sled	3 point belt and airbag	Impact speed=50km/h, belt load limit=4kN
10	HUMOS	Sled	3 point belt and airbag	Impact speed=60km/h, belt load limit=4kN
11	HUMOS	Pendulum	Hub impactor	Impactor mass =23.4 kg, impact speed=4.3m/s
12	HUMOS	Pendulum	Hub impactor	Impactor mass =23.4 kg, impact speed=5.0m/s
13	HUMOS	Pendulum	Hub impactor	Impactor mass =23.4 kg, impact speed=5.9m/s
14	HUMOS	Static	Airbag only	Depowered airbag #1*
15	HUMOS	Static	Airbag only	Depowered airbag #2*
16	HUMOS	Sled	Airbag only	Impact speed=40km/h
17	HUMOS	Sled	Airbag only	Impact speed=45km/h
18	HUMOS	Sled	Airbag only	Impact speed=50km/h

\*In condition 1 and 2 the impactor is 178mm and 128mm, respectively, away from subject

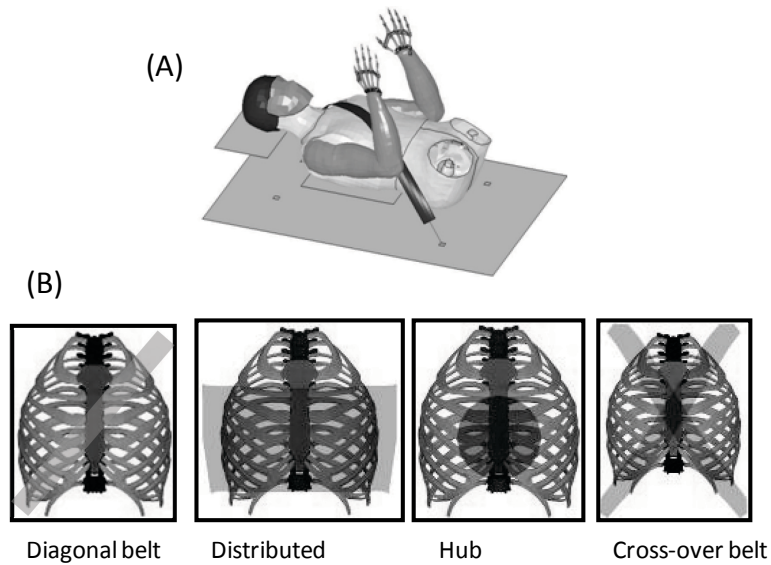


Figure 4: Overview of the THUMS torso model orientation (A) and four different restraints considered with the THUMS model in this study (B).

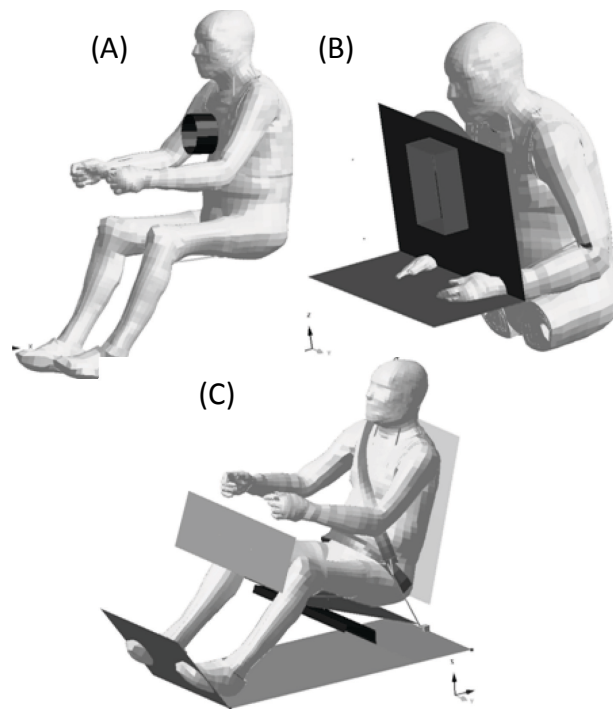


Figure 5: Overview of the different HUMOS model orientation (A) Static pendulum impact test, (B) static airbag tests, (C) dynamic sled test with belt and/or airbag.

*Multi-point deflection and strain measurements.* Nine deflection measurement locations were identified on the human thorax models to characterize the multi-point deflection observed during the thoracic deformation (Figure 6). The nine locations included four points on the anterior thorax at the 4<sup>th</sup> and 8<sup>th</sup> rib level corresponding to the four-point deflection instrumentation available in the THOR ATD. The location of the deflection measurement along the curvature of these ribs (4<sup>th</sup> and 8<sup>th</sup>) was adjusted to avoid the effects of the local stress concentration due to the presence of the costal-cartilage joints. In addition to the four anterior deflection locations, two lateral rib locations were identified on the 4<sup>th</sup> and the 8<sup>th</sup> rib. The co-ordinates of the

location corresponded to the mid-point of the rib's curvilinear axis originating from the vertebrae and ending at the costal-cartilage joint. The estimate the multi-axis deflections (x,y, and z) at these eight locations, two local coordinate systems (LCS) were identified at the T4 and T8 vertebrae, respectively. The two LCS's were defined such that the x and y components of the deflection were measured in the two rib planes at the 4<sup>th</sup> and the 8<sup>th</sup> rib level. The origin of each of the LCS was at the center of the vertebrae, with the principal x-axis defined as the line joining the origin and the mid-point of the left and right rib's anterior extremities. The y-axis was defined as the line joining the center of the transverse processes of the vertebrae. Finally, deflection was also measured at the mid-sternum location, corresponding to the deflection instrumentation available on the Hybrid-III ATD. The LCS for the mid-sternum deflection involved an origin at the T8 vertebrae with the principal x-axis joining the origin and the mid-sternum location. The y-axis for this LCS was defined in the same manner as the LCS y-axis at the T8 vertebrae. The measurement locations and the LCS definitions are illustrated in Figure 6. The peak first principal strain was estimated at each rib level (separate for left and right aspect). The deflection at the nine locations and the strains were both sampled at 1 kHz.

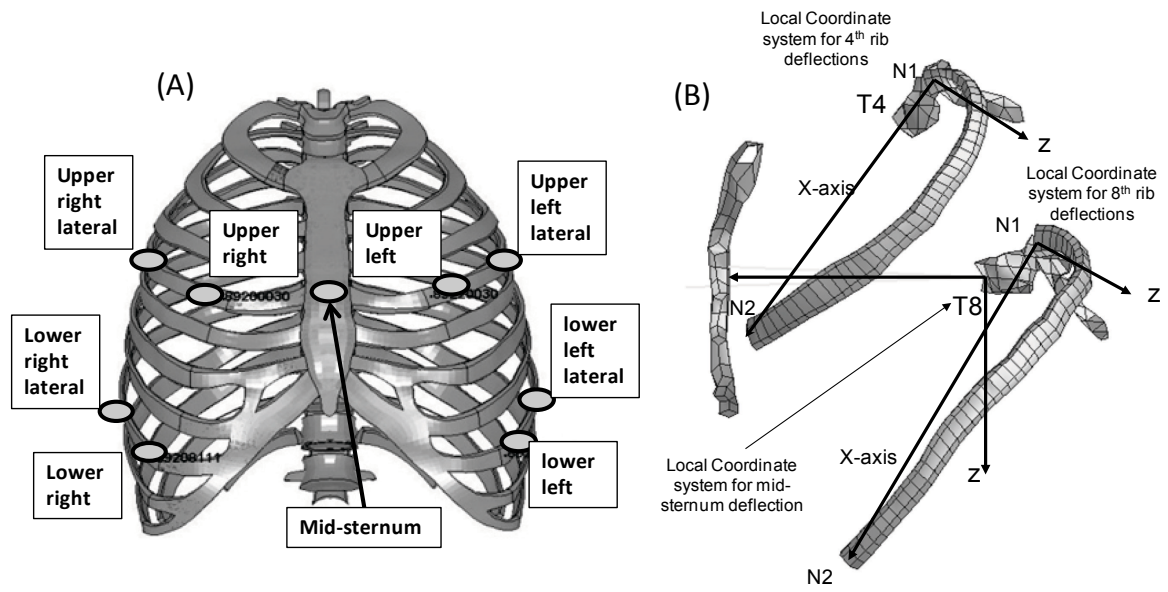


Figure 6: Schematic showing, (A) location of the multi-point deformation measurements, and (B) definition of local coordinate systems defined for the measurement of mid-sternum and 4<sup>th</sup> and 8<sup>th</sup> rib deflections.

## Statistical Analysis

Several multivariate analyses were performed on the injury deflection data samples collected from the PMHS experimental tests and the computation simulations described in the previous sections. The objective of these analyses as outlined before was to identify important multi-point based deflection predictors for thoracic injury risk and analyze the sensitivity of the injury prediction to covariates such as the restraint type. The analyses steps are summarized below.

1. Logistic regression models were developed using results from the twenty PMHS sled tests. Linear combinations of peak resultant deflections (resultant of x and y deflection components) at the six measurement locations were used as the explanatory variables to predict the risk of thoracic injury. The predictor variables, based on composite deflection measures, included the peak mid-sternum deflection, maximum deflection measured at any of the six locations ( $C_{max}$ ), the peak sum of deflections measured on the three points on the upper and lower chest-bands, the sum of deflections measured at the six locations at the time of  $C_{max}$ , the overall maximum of deflections measured at the four lateral locations (corresponding to the CRUX locations) and at all the six locations. The seven predictor variables correspond to seven univariate regression models ( $n= 20$  in each model) with binary outcome characterized by the incidence of AIS 3+ injury.

2. The predictors of the seven regression models were compared to each other based on their Goodness-of-fit to the model, predictability of outcome and significance of the regression coefficients. The statistical measure used to quantify and compare the Goodness-of-fit measure across the seven models was the Akaike Information Criteria (AIC). The predictability of outcome was quantified in each of the models by estimating the area under the Receiver Operator Characteristic (ROC) curve and the Goodman Kruskal's Gamma measure. The significance of the regression model coefficients were compared by the p-value estimated for the predictor variable.
3. Linear regression model was developed using results from the 18 simulations corresponding to a variety of different representative loading conditions (refer to Table 1 for details) and human models. The strain-deflection dataset sampled at 1 kHz from each of the 18 simulations provided a total of 1552 independent data samples. The independent data samples assume that the strain development in the thoracic ribs is independent on the time-history of the thoracic deflection. The injury predictor variables included seven quantifiable deflection-based explanatory variables and seven qualitative co-variables represented in the regression model. The seven deflection predictors were resultant deflection (x and y components) measured at the mid-sternum, each of the four frontal locations (upper left, upper right, lower left lower right) and the sum of lateral deflections (left and right) measured at the 4<sup>th</sup> and the 8<sup>th</sup> rib level. The seven qualitative variables represented the loading condition type (ordinal: 1 to 18), model type (ordinal: THUMS or HUMOS), and the incidence of belt loading, airbag loading, hub loading, load limiting restraint type, and sled test. The outcome variable was the overall peak of first principal strain measured on the rib cage. In summary, the linear regression model had 14 predictor variables and one continuous outcome variable.
4. A stepwise regression procedure was used to identify significant predictor variables in the model. Predictors were included in the model if the F-statistic for the variable to be added was significant at  $p < 0.05$ . At each iteration if any of the variables already included in the model was not significant at  $p < 0.05$  then it was excluded from the model. Statistical measures such as the regression coefficients, standard error, F statistic p-value, were computed for each of the predictor retained in the model.
5. To further investigate the correlation between the multi-point deflection components, the Pearson's correlation coefficients were estimated for each of the pair wise deflection predictors. In addition to the correlation coefficients, the Principal Component Analysis (PCA) of the deflection predictors and an analysis of the common factors were performed in this study. The principal components of the multi-point deflection described the minimum number of Eigen vectors required to explain the total variance in the model. Further, a common factor analysis was performed to estimate the minimum number of factors to explain the common variance among the observed deflection variables. To determine if the common factor model is appropriate for the multi-point deflection, Kaiser's Measure of Sample Adequacy (KMSA) was calculated for each deflection component. A scree plot of the Eigen values was used to determine the appropriate number of common factors in the model. The results of the principal component analysis and the common factor analysis provided insight towards minimizing the redundancy in the multi-point deflection in predicting the risk of thoracic rib injury.

## **RESULTS AND DISCUSSION**

### **PMHS injury-deflection correlation**

Logistic regression models developed based on PMHS sled test data compared the performance of individual deflection predictors to distinguish injurious (AIS 3+) and non-injurious loading conditions. The output of the regression models was expression as a cumulative probability density function or commonly known as the injury risk function. For instance, Figure 7 shows the injury risk curve (with 95% confidence intervals) for mid-sternum deflection as the predictor variable and the incidence of AIS 3+ rib injury as the binary outcome. The injury risk curves for the remaining composite deflection predictors are shown in Figure A. 1. It should be noted that the regression assume an underlying logistic distribution function for the injury outcome. Additionally, the deflection measurement at injury outcome is censored in these tests as the exact timing of the injury during the test is not known. Therefore, the deflection magnitudes corresponding to the risk of injury is expected to be biased as regression models do not account for the censored characteristic of

the data points. The purpose of developing the regression models is, however, to compare the performance of the predictors rather than evaluate deflection measurements for injury risk.

The statistical measures quantifying the predictability, Goodness-of-fit, and the statistical significance of the regression coefficients were compared for each of the predictor variables (Table 2). The AIC measure indicated that the mid-sternum deflection and the  $C_{max}$  (among all six locations) were the two top ranked predictors in terms of Goodness-of-fit of the regression model. Similarly, the mid-sternum deflection and the  $C_{max}$  measure were also the top ranked predictors in terms of predictability (measured by Kruskal's Gamma and the area under the ROC curve) and significance of regression coefficients (Wald chi-square p-value). The overall results from the PMHS sled tests with occupant restrained by 3-point belt loading indicated that the mid-sternum deflection and the  $C_{max}$  measure were better predictors compared to other composite deflection measures considered in this study.

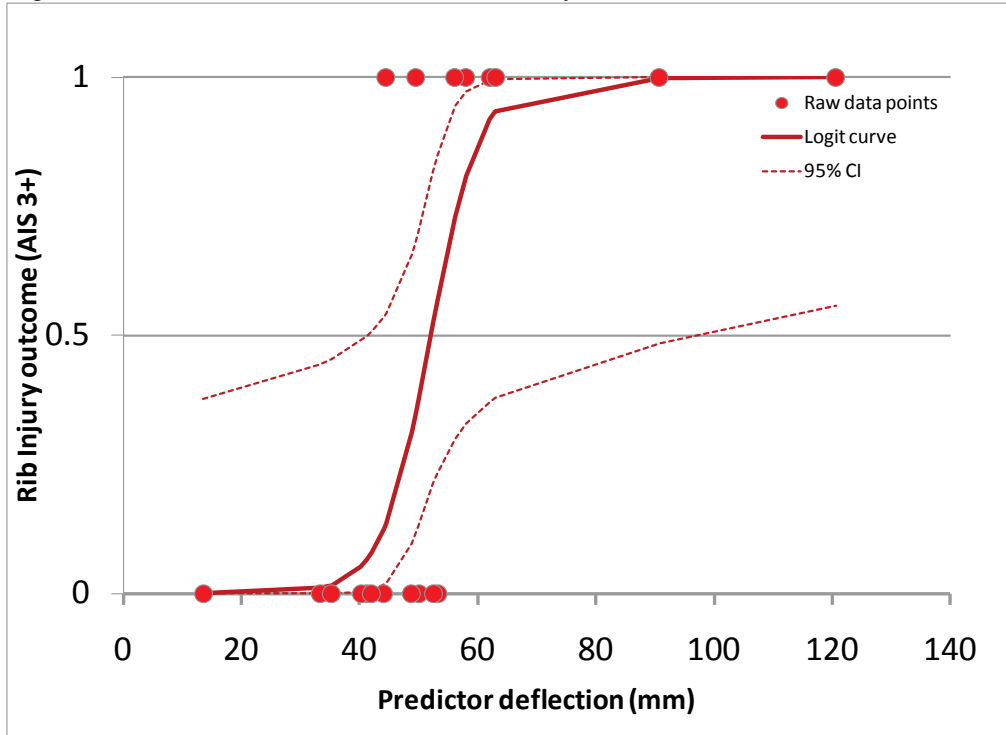


Figure 7: Logistic regression for mid-sternum deflection as predictor for AIS 3+ rib injury.

Table 2: Statistical measures comparing Goodness-of-fit, predictability, regression coefficients and deflection at 50% injury risk.

Predictors	AIC	Kruskal Gamma	ROC area	Wald chi-square	p-value	Deflection at 50% risk (mm)
Mid Sternum	17.073	0.84	0.92045	4.12	0.042	52
Cmax (6 point)	16.494	0.81	0.9074	3.27	0.071	56
Lower band sum	19.826	0.75	0.87302	3.45	0.063	21
Upper band sum	19.573	0.71	0.85227	3.49	0.062	49
6-point sum at Cmax	23.93	0.68	0.84127	2.63	0.105	187
4-point sum (overall)	20.739	0.56	0.77778	2.50	0.114	117
6-point sum (overall)	21.857	0.56	0.77778	2.19	0.139	191

## Simulation based strain deflection correlation

The results of the stepwise linear regression model yielded 10 significant predictor variables (seven deflection predictors and three qualitative predictors, Table 3) for the estimation of peak overall strain in the thorax model when deformed in 18 different loading conditions. The regression model included 1522 data samples with an overall F-statistic of 128.8 ( $p < 0.0001$ ). Among the qualitative predictors representing the loading environment, the presence of belt loading and choice of the human model were not significant in the correlation between the deflection measures and the peak strain outcome. The presence of airbag and hub loading, and load-limiting restraining force, however, were influential ( $p < 0.05$ ) in the prediction of strain outcome. Among the deflection predictors, all seven components representing anterior and lateral deflections at the 4<sup>th</sup> and the 8<sup>th</sup> rib level were significant ( $p < 0.05$ ) for the prediction of overall strain in the model in the given range of loading conditions analyzed in this study. In the overall model, 46% of the variance was explained by the predictors as indicated by the R-Squared measure. For each predictor variable in the model, the regression co-efficient, standard error, Wald Chi-Squared F-value and the co-efficient p-value, are presented in Table 3.

The Pearson product-moment correlation matrix indicated the pair-wise degree of linear Collinearity among the deflection predictors (

Table 4). The Pearson's Correlation co-efficient for all pairs of deflection predictors were positive and significant at  $p < 0.05$ . The highest degree of correlation ( $r = 0.96$ ) was observed for upper left (4<sup>th</sup> rib) and upper lateral (sum of lateral deflections at 4<sup>th</sup> rib). The second highest correlation was observed between lower right (8<sup>th</sup> rib) and lower lateral (sum of lateral deflections at 8<sup>th</sup> rib), and the remaining pairs exhibited a correlation coefficient,  $r$  less than 0.90.

The results of the PCA indicated that a single large Eigen value (5.66) explained for 81% of the standardized variance in the model. The next largest Eigen value was 0.5 which cumulatively explained for 89% of the standardized variance. The largest Eigen Factor (5.66) had positive loading (range: 0.86-0.93) for all seven deflection predictors. Further, results from the common factor analysis showed that the KMSA measure for each of the deflection predictors ranged from 0.81 to 0.89 indicating that the partial correlations are significantly different from the original correlation coefficients (Figure 9). The scree plot of the Eigen values obtained from the common factor analysis indicate three factors which account for almost 100% of the common variance (Figure 8). The factor pattern suggests that while the first factor explains for maximum variance (5.56), the variance explained by the second and the third factor is substantially low (0.44 and 0.24, respectively). All seven deflection predictors had large loadings (range: 0.83 to 0.98) on the first factor (Figure 9). The results from the common factor analysis indicates that a single underlying factor is responsible for the correlation between the multi-point deflections and the maximum overall strain measured in the rib cage.

Table 3: Regression results for multipoint deflections as predictor for overall peak strain.

Model selection: stepwise method (entry and retain criteria =  $p < 0.005$ )  
 Sample size 1552  
 F-value (p-value) 128.83 ( $< 0.0001$ )  
 R-Square 0.4553

Predictors	Regression Co-efficient	Standard error	F-value	p-value
Mid-sternum	0.003	0.000	42	<.0001
Upper left	-0.004	0.001	7	0.0079
Upper right	0.012	0.001	155	<.0001
Lower left	-0.012	0.001	128	<.0001
Lower right	-0.011	0.001	63	<.0001
Upper lateral	-0.003	0.001	7	0.0079
Lower lateral	0.009	0.001	63	<.0001
Airbag	-0.057	0.010	31	<.0001
Hub	-0.071	0.015	24	<.0001
Load limiter	0.023	0.010	5	0.0229

Table 4: Correlation matrix for the multi-point deflection components under all loading conditions

	Mid-Sternum	Upper Left	Upper Right	Lower Left	Lower Right	Upper Lateral	Lower Lateral
Mid-Sternum	1.00	0.74	0.87	0.70	0.76	0.72	0.77
Upper Left	0.74	1.00	0.87	0.74	0.71	0.96	0.75
Upper Right	0.87	0.87	1.00	0.67	0.72	0.87	0.70
Lower Left	0.70	0.74	0.67	1.00	0.73	0.73	0.86
Lower Right	0.76	0.71	0.72	0.73	1.00	0.77	0.90
Upper Lateral	0.72	0.96	0.87	0.73	0.77	1.00	0.77
Lower Lateral	0.77	0.75	0.70	0.86	0.90	0.77	1.00

All estimates are significant at  $p < 0.0001$

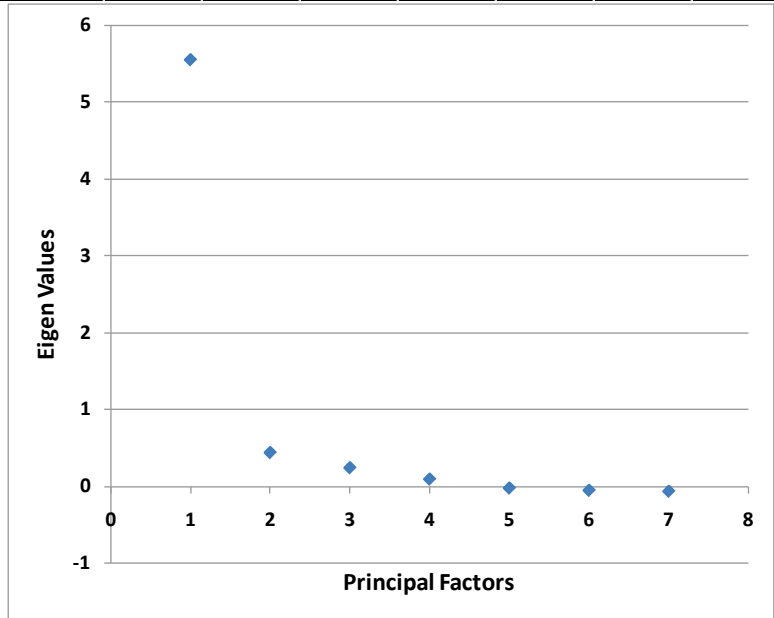


Figure 8: Scree plot for the eigen values determined through the principal factor analysis

Figure 9: Factor Pattern Analysis and Kaiser's Measure of Sampling Adequacy (KMSA) for each of the multi-point deflection components.

	Factor Pattern			KMSA
	Factor 1	Factor 2	Factor 3	
Mid-Sternum	0.93	-0.24	-0.20	0.82
Upper Left	0.92	-0.28	-0.17	0.81
Upper Right	0.91	0.34	-0.07	0.84
Lower Left	0.90	-0.27	0.21	0.89
Lower Right	0.88	0.27	0.04	0.80
Upper Lateral	0.87	0.01	0.33	0.79
Lower Lateral	0.83	0.20	-0.13	0.79
Overall	5.55	0.44	0.24	0.82

## CONCLUSIONS

Statistical correlation between multi-point thoracic deflection and risk of rib injury was estimated using results from experimental PMHS sled tests and computational simulation of thoracic deformation. In cases of PMHS subjects in frontal sled tests restrained by 3-point belt system, the mid-sternum deflection and  $C_{max}$  measure were identified as reliable predictors of severe injury risk to the thorax. The restraint condition for the PMHS sled test was however limited to the 3 point safety belt only. Using computational simulation of thoracic deformation under 18 different loading conditions, a linear regression model expressing peak strain in the thoracic as a function of deflection predictors was determined. Seven variables including resultant deflections measured at the anterior and lateral part of the ribcage (at 4<sup>th</sup> and 8<sup>th</sup> rib levels) and mid-sternum locations were significantly correlated to the maximum strain in the overall rib cage. The regression model exhibited dependence (significant at  $p < 0.05$ ) on certain restraint related qualitative parameters including presence of airbag loading, hub impact and load-limiting restraint force. The multi-point deflections were further analyzed for correlation, principal components and underlying common factors. The Pearson's coefficients indicated highest degree of position correlation between the anterior left deflection on the 4<sup>th</sup> rib and the sum of lateral deflections at the same level ( $r=0.96$ ). Results of both, PCA and Common Factor Analysis, indicated that the first Eigen vector was responsible for the 81% of the overall variance among the deflection predictors. Further insight into the non-linear interaction between the multi-point deflection measurements is necessary to develop a regression function which is independent of the restraint related parameters.

## ACKNOWLEDGEMENTS

We would like to acknowledge NHTSA's Research and Development Program for providing both research direction and financial support.

## REFERENCES

- AAAM (2005). The abbreviated injury scale -2005. [report] Association for the Advancement of Automotive Medicine, Des Plains, IL
- BOSE, D., PIPKORN, B., CRANDALL, J. R., LESSLEY, D., J., TROWBRIDGE, M. J., (2009). Multi-point Thoracic Deflection Measurement as a Predictor of Rib Injury in Frontal Collision. Proc. 37<sup>th</sup> International Workshop on Human Subjects for Biomechanical Research. Phoenix, USA.
- EPPINGER, R., SUN, E., BANDAK, F. et al., (1999) Development of improved injury criteria for the assessment of advanced automotive restraint systems-II. [report] National Highway Traffic Safety Administration, U.S. Department of Transportation, Washington, DC.
- KENT, R., LESSLEY, D., SHERWOOD, C., (2004). Thoracic response to dynamic, non-impact loading from a hub, distributed belt, diagonal belt, and double diagonal belts. Stapp Car Crash Journal, 48.
- KROELL, C., SCHNEIDER, D. and NAHUM, A. (1971) Impact tolerance of the Human Thorax 1. Proc. 15<sup>th</sup> Stapp Car Crash Conference, pp. 84-134. Society of Automotive Engineers, Warrendale, USA.
- KROELL, C., SCHNEIDER, D. and NAHUM, A. (1974) Impact tolerance of the Human Thorax 2. Proc. 18<sup>th</sup> Stapp Car Crash Conference. Society of Automotive Engineers, Warrendale, USA.
- KUPPA S. and EPPINGER, R., (1998). Development of an improved thoracic injury criterion, Stapp Car Crash Journal, pp. 139-153.
- LEBARBE, M., POTIER, P., BAUDRIT, P., PETIT, P., TROSSEILLE, X., and VALLENCIEN, G. (2005) Thoracic Injury Investigation using PMHS in Frontal Airbag Out-of-Position Situations. Stapp Car Crash Journal, Vol. 49 (November 2005).
- LI, Z., KINDIG, M. W., KERRIGAN, J. R., UNTAROIU, C. D., SUBIT, D., CRANDALL, J. R., KENT, R. W., (2010). Rib Fractures under anterior-posterior dynamic loads: Experimental and finite-element study. J. Biomechanics, Vol. 43, pp-228-234.

- MURAKAMI, D., KITAGAWA, Y., KOBAYASHI, S., KENT, R., and CRANDALL, J. (2004). Development and Validation of a finite element model of a vehicle occupant. Proc. Society of Automotive Engineers World Congress, Detroit, Michigan.
- OSHITA, F., OMORI, K., NAKAHIRA, Y., & MIKI, K. (2002). Development of a finite element model of the human body. 7th International LS-Dyna Users Conference, Nagoya, Japan. , 1 37-48
- PETITJEAN, A., LEBARBE, M., POTIER, P., TROSSEILLE, X. and LASSAU, J-P. (2002) Laboratory Reconstructions of Real World Frontal Crash Configurations using the Hybrid III and THOR Dummies and PMHS. Stapp Car Crash Journal, Vol. 46 (November 2002), pp: 27-54.
- SONG, E., TROSSEILLE, X., and BAUDRIT, P. (2009) Evaluation of Thoracic Deflection as an Injury Criterion for Side Impact Using a Finite Elements Thorax Model. Stapp Car Crash Journal, Vol. 53 (November 2009), pp: 155-191.
- VEZIN, P. and VERRIEST, J.P. (2005) Development of a set of numerical human model for safety. Proc. of the 19th Int. Tech. Conf. on the Enhanced Safety of Vehicles, Paper Number (05-0163)

## APPENDIX

Table A.1. Summary of PMHS subjects used for chest-band analysis

Test ID	Impact speed	Age	Gender	Mass	Height	BMI	Chest depth	Restraint	Force limiting belt	Pretensioner belt	No. of rib fx.	AIS
	(km/h)	(year)		(kg)	(m)	(kg/m <sup>2</sup> )	(mm)					
1094	29.9	49	M	58.1	1.78	18	226	3point belt	No	No	0	0
1095	29.8	44	M	77.1	1.72	26	226	3point belt	No	No	0	0
1096	29.5	39	M	79.4	1.84	23	260	3point belt	No	No	0	0
1262	48.9	51	M	54.9	1.75	18	205	3point belt	No	No	13	4
1263	47.1	57	F	108.9	1.65	40	252	3point belt	No	No	29	4
1264	48.5	57	M	59.0	1.79	18	210	3point belt	No	No	13	4
1386	48.0	67	M	71.0	1.75	23	231	3point belt	Yes	Yes	12	4
1387	48.0	69	M	60.0	1.71	21	230	3point belt	Yes	Yes	2	1
1389	48.0	72	M	73.0	1.75	24	265	3point belt	Yes	Yes	17	4
1110	39.2	44	M	77.1	1.72	26	223	3point belt	No	No	0	0
1332	29.0	54	M	124.3	1.89	35	293	3point belt	Yes	Yes	0	0
1333	48.0	54	M	124.0	1.89	35	269	3point belt	Yes	Yes	7	3
1334	29.0	53	M	151.0	1.82	46	345	3point belt	Yes	Yes	0	0
1335	48.0	53	M	151.0	1.82	46	322	3point belt	Yes	Yes	2	2
1384	29.0	54	F	27.2	1.47	13	194	3point belt	Yes	Yes	0	0
1385	48.0	54	F	27.2	1.47	13	195	3point belt	Yes	Yes	2	2
1388	48.0	54	F	27.2	1.47	13	177	3point belt	No	No	7	3
1427	48.3	72	M	87.5	1.73	29	276	3point belt	Yes	Yes	7	4
1428	48.3	69	M	69.4	1.75	23	241	3point belt	Yes	Yes	0	0
1429	48.4	40	M	83.0	1.86	24	239	3point belt	Yes	Yes	2	2

Figure A. 1: Logistic regression results for rib injury prediction based on chest-band deflections

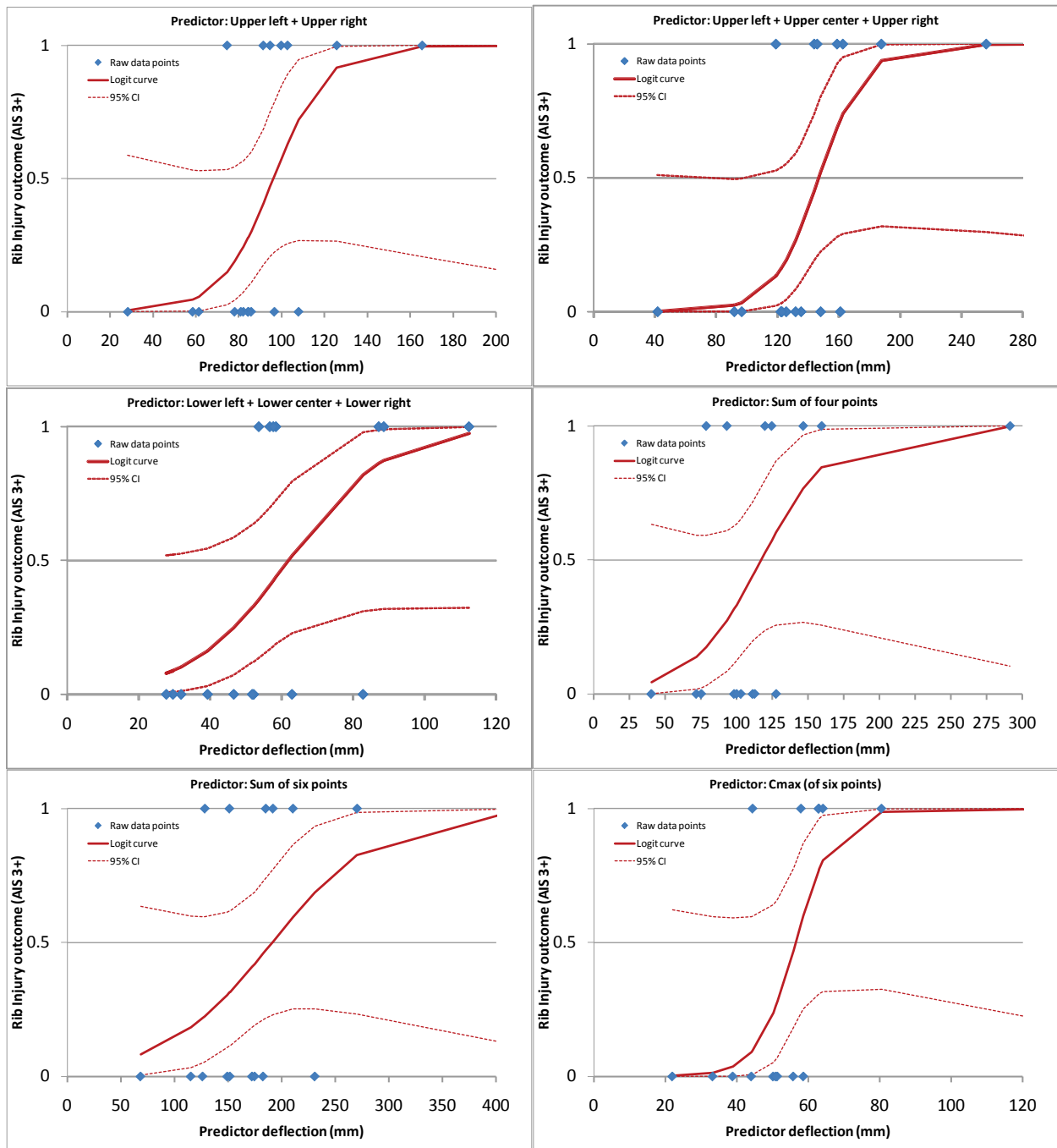
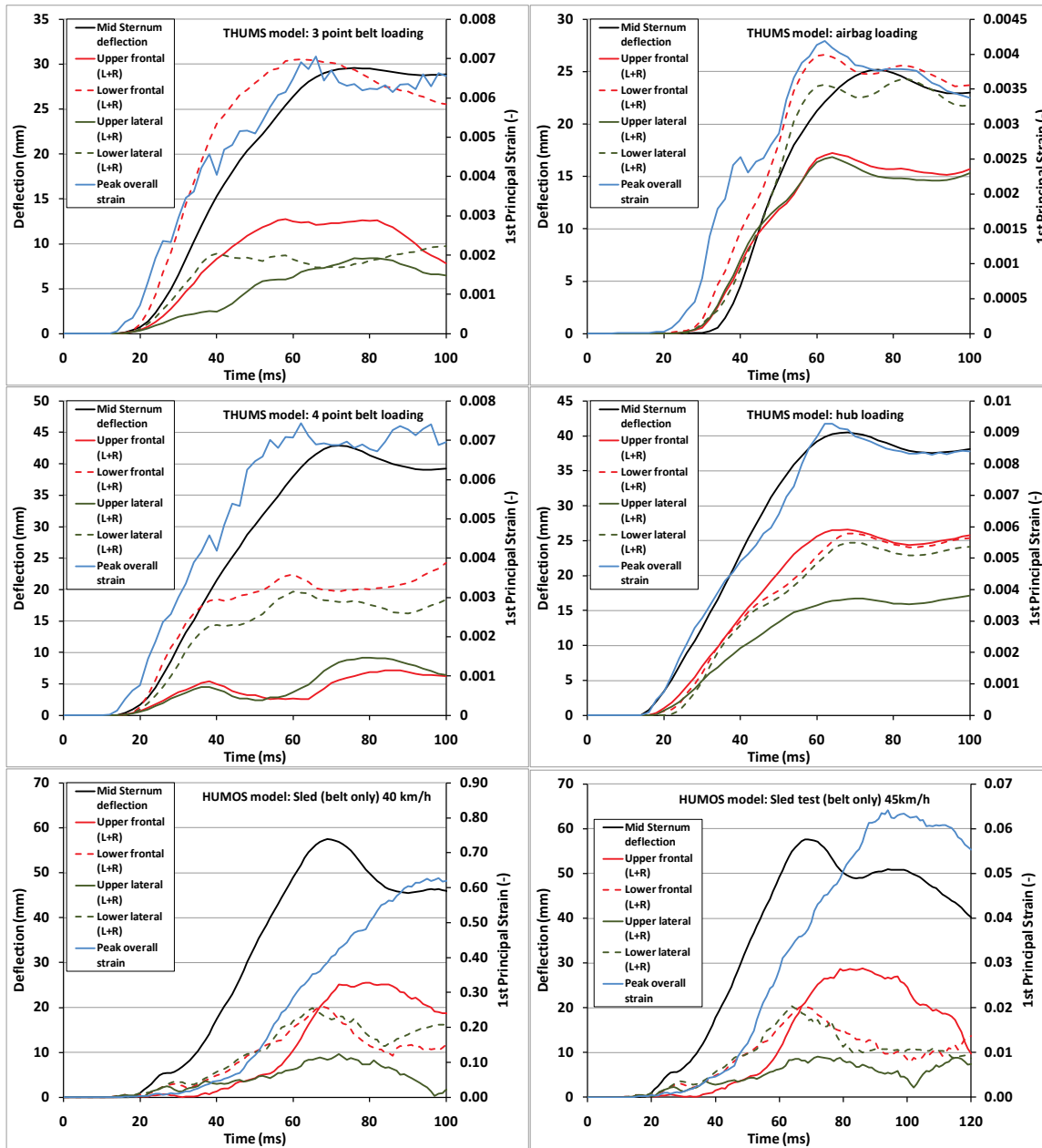
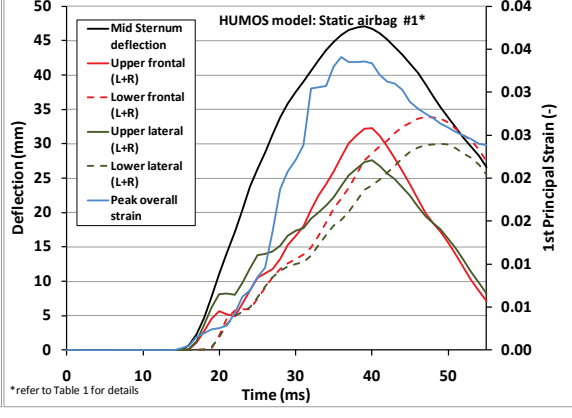
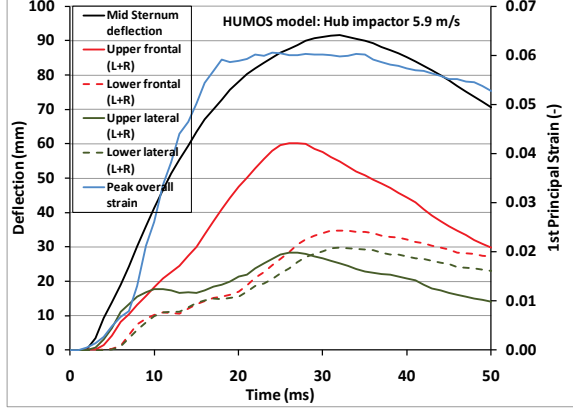
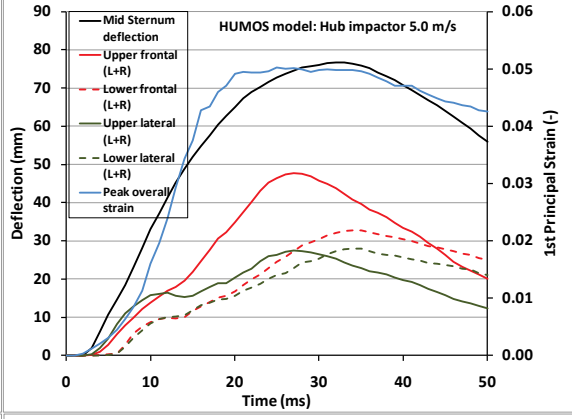
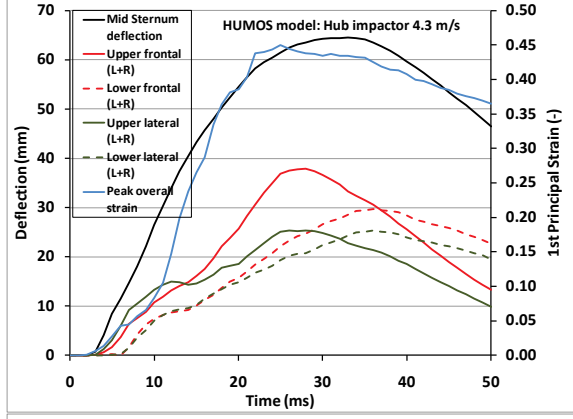
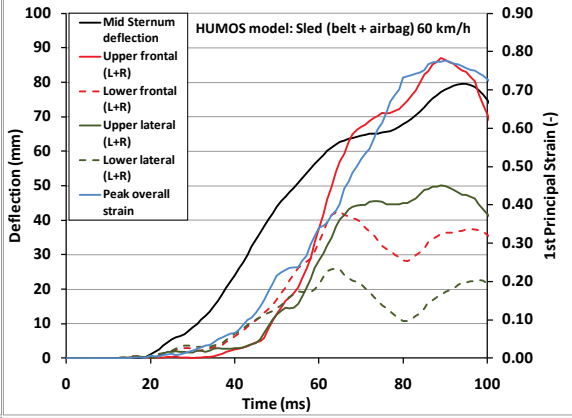
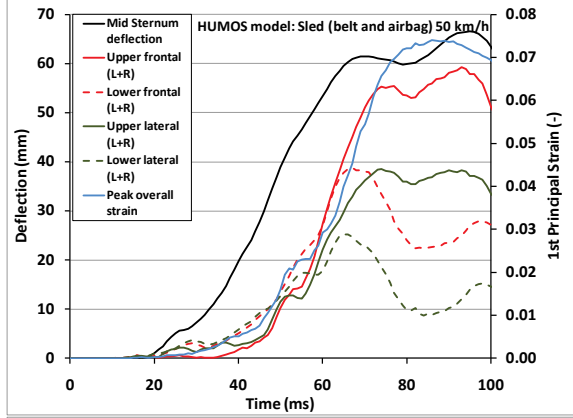
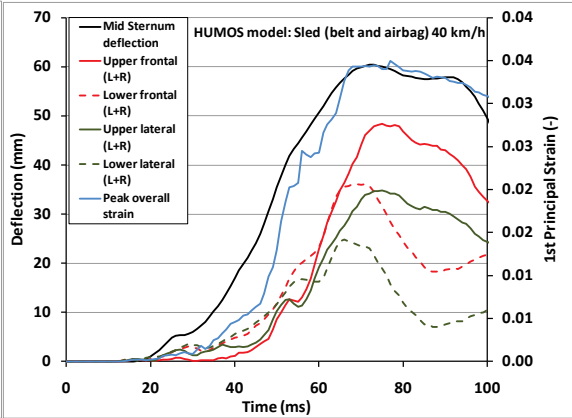
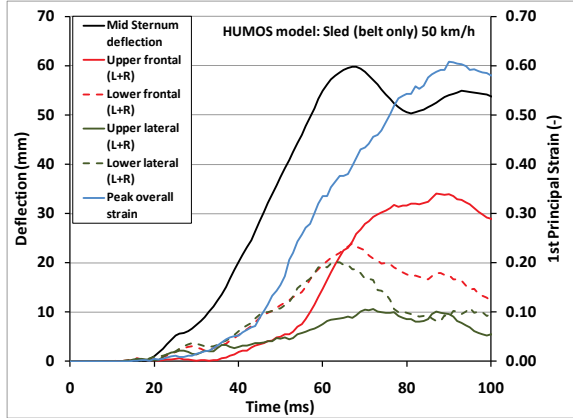
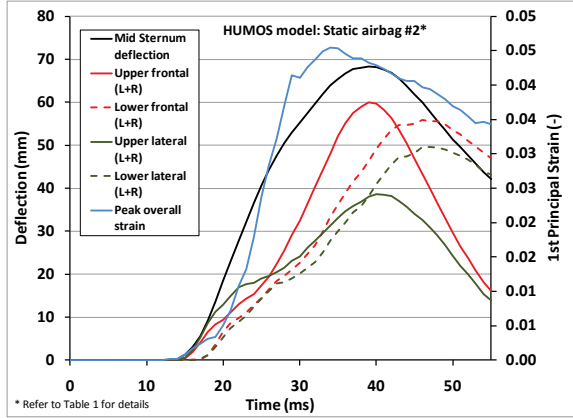


Figure A.2 Deflection and strain time history for thoracic deformation simulated with the human FE models.





\*refer to Table 1 for details



\* Refer to Table 1 for details

